HST Observations of Neutron-Capture Elements in Very Metal-Poor Stars

Christopher Sneden,[1] John J. Cowan,[2] Debra L. Burris,[2] and James W. Truran[3]

chris@verdi.as.utexas.edu, cowan@mail.nhn.ou.edu, burris@mail.nhn.ou.edu, truran@nova.uchicago.edu

ABSTRACT

Using the Goddard High Resolution Spectrograph (GHRS) of the Hubble Space Telescope (HST) we have detected the neutron-capture elements osmium, platinum, and lead in the very metal-poor ([Fe/H] $\simeq -2.8$) Galactic halo star HD 115444. This star joins the metal-poor giant HD 126238 ([Fe/H] $\simeq -1.7$) as the second Galactic halo star for which "$3^{\rm rd}$ neutron-capture peak" elements have been detected. We have also determined upper limits on these same elements for the neutron-capture deficient star HD 122563 ([Fe/H] $\simeq -2.7$). We have identified zirconium and germanium features in the HST spectra of all three stars; this marks the initial identification of the latter element in halo stars.

We compare and contrast the spectra and abundances of the neutron-capture elements in these three stars. Combining the new HST observations of the $3^{\rm rd}$ neutron-capture peak elements of HD 115444 with ground-based data, we find the stellar abundance distribution, over a wider atomic number range than ever before possible, is consistent with the solar system r-process abundance curve. Comparison of this star with the more metal-rich HD 126238 finds that the ratio of the $3^{\rm rd}$-peak element abundances to that of the pure r-process element europium is *same in both stars.* Earlier ground-based studies have found that abundances of the lighter elements, such as barium and europium, in HD 115444 exceed those of HD 122563 by ~ 0.7 dex. Our osmium, platinum, and lead upper limits show a similar difference and are not inconsistent with either the scaled solar r-process or the solar total distribution. Thus, the $2^{\rm nd}$ and $3^{\rm rd}$ neutron-capture peak element ($Z \geq 56$) abundances in all three stars are consistent with scaled solar system r-process abundances. However, the zirconium abundance is approximately the same in HD 122563 and HD 115444,

---

[1]Department of Astronomy and McDonald Observatory, University of Texas, Austin, TX 78712

[2]Department of Physics and Astronomy, University of Oklahoma, Norman, OK 73019

[3]Department of Astronomy and Astrophysics, University of Chicago, Chicago, IL 60637

so this element (near the 1st neutron-capture peak) is overabundant (somewhat) in HD 122563 and (slightly) in HD 115444 with respect to the solar *r*-process abundances. Germanium (synthesized in approximately equal amounts by the *r*- and the *s*- process in solar material) is underabundant in all three stars, but does seem to scale with metallicity – it is identical in HD 115444 and HD 126238, but significantly greater in the higher metallicity HD 126238. These new results support previous observations that demonstrate the operation of the *r*-process, including the synthesis of the heaviest such elements, early in the history of the Galaxy. Implications of these results for early Galactic chemical evolution are discussed.

Subject headings: Galaxy: evolution — nuclear reactions, nucleosynthesis, abundances — stars: abundances — stars: individual (HD 115444, HD 126238, HD 125268) — stars: Population II

1. Introduction

The abundances of neutron-capture elements (those with atomic numbers Z > 30) in the oldest, metal-poor halo stars contain vital clues to unlocking the secrets of the early chemical history and evolution of the Galaxy. Since the halo stars seen today must have been formed near the beginning of the Galaxy, out of ejecta from a previous generation of stars, the neutron-capture element abundances can be used to determine the initial Galactic conditions and nature of the nucleosynthetic processes shortly after Galactic time zero. Abundances of several neutron-capture elements that are produced in *s*(*low*)- and *r*(*apid*)-neutron-capture processes may be determined in very metal-poor stars. While observational and theoretical studies (*e.g.*, Spite & Spite 1978, Truran 1981, Sneden & Parthasarathy 1983, Sneden & Pilachowski 1985, Gilroy *et al.* 1988, Gratton & Sneden 1994, McWilliam *et al.* 1995) have used these abundances to demonstrate that *r*-process production occurred early in the history of the Galaxy, it has been difficult to accurately assess the nature and extent of such processing. There have been two primary difficulties. First, only a few neutron-capture elements have transitions easily accessible to ground-based spectroscopy. None of these detectable elements lies directly at a solar system *r*-process peak. It is especially frustrating that abundances of the important heavy elements comprising the 3rd, most massive (mass number A $\sim$ 200) peak such as Os, Ir, and Pt are virtually unknown for metal-poor stars. Second, even the few routinely detectable neutron-capture elements usually present only a handful of transitions for analysis. For many species (*e.g.*, Ce II, Gd II) the transitions are all so weak that feature identification and abundance derivation have large uncertainties. For two key species (Sr II and Ba II) there is the opposite problem: their transitions almost always are so strong that uncertainties in atmospheric modeling and in hyperfine/isotopic line substructure yield large uncertainties in abundance analyses.

Knowledge of neutron-capture elements in early Galactic halo stars has been bolstered by the recent discovery and extensive spectral analysis of CS 22892-052, an ultra-metal-poor ([Fe/H]$\simeq -3.1$[4]) yet very neutron-capture-rich star that was a serendipitous discovery of the McWilliam *et al.* (1995) abundance survey of very low metallicity stars. Sneden *et al.* (1994) and Cowan *et al.* (1995) conducted initial studies of the CS 22892-052 abundance trends. Recently, Sneden *et al.* (1996) have used high resolution, high signal-to-noise (S/N) data to explore the CS 22892-052 spectrum, determining abundances of 20 neutron-capture elements in this star. Some of these elements (such as terbium, holmium, thulium and hafnium) had never previously been detected in metal-poor halo stars.

All analyses of CS 22892-052 have employed ground-based spectra. Most of the elements detected in this and all other metal-poor stars have been the rare-earths, which are elements between the 2$^{\rm nd}$ (dominated by Te and Xe) and 3$^{\rm rd}$ (containing the elements Os, Ir and Pt) *r*-process neutron-capture peaks. The second and third *s*-process peaks occur at mass numbers slightly higher than the *r*-process peaks, and are dominated by the abundances of Ba and Pb, respectively. In contrast, the least massive 1st *s*- and *r*-process neutron-capture peaks, defined by elements such as Se, Kr and Sr and Zr – the latter two detected in CS 22892-052 by Sneden *et al.* (1996) – show a large overlap in mass number from $\sim$ 80-90.

Cowan *et al.* (1997a) have used the rare-earth abundances together with that of the radioactive cosmochronometer element thorium to deduce an age for CS 22892-052. The long-lived radioactive elements in the uranium-thorium region, are synthesized in the *r*-process. Thus, comparison of the thorium abundance in CS 22892-052 with that at the time of formation in an *r*-process site provides a direct radioactive-decay age estimate for this star. Such a comparison depends critically upon ascertaining the abundances of the stable 3rd *r*-process-peak elements, with atomic numbers relatively near thorium. The age determination of CS 22892-052 by Cowan *et al.* (1997a) was hampered by the lack of reliable abundances of 3$^{\rm rd}$ *r*-process-peak elements. We still know little about 3$^{\rm rd}$-peak abundances in metal-poor stars, and unfortunately the situation is unlikely to change soon even for CS 22892-052, since its visual magnitude is 13. We must turn to brighter stars, such as the ones presented in this paper, to gain further insights on the heaviest stable elements.

In HST Cycles 4, 5, and 6 we have used the Goddard High Resolution Spectrometer (GHRS) to search for strong *UV* transitions of 3$^{\rm rd}$-peak elements in three very metal-poor giant stars: HD 122563, HD 126238, and HD 115444. Cowan *et al.* (1996) have reported detections of osmium, platinum, and lead in HD 126238. In this paper we discuss the complete GHRS data for all three stars. In §2 we describe the GHRS observations. The spectra are inter-compared in §3, along with a discussion of the chosen transitions and their atomic parameters. The abundance analysis is given in §4, and in §5 we conclude with a discussion of our results.

---

[4]We adopt the usual spectroscopic notations that $[{\rm A/B}] \equiv \log_{10}({\rm N_A/N_B})_{\rm star} - \log_{10}({\rm N_A/N_B})_{\odot}$, and that $\log\,\epsilon({\rm A}) \equiv \log_{10}({\rm N_A/N_H}) + 12.0$, for elements A and B. Also, metallicity will be arbitrarily defined here to be equivalent to the stellar [Fe/H] value.

2. Observations and Reductions

We observed three very metal-poor giant stars for this program. Preliminary predictions of the *UV* spectra for a variety of metal-poor stars suggested that the strengths of 3rd neutron-capture peak transitions simply would be too weak for detection in main sequence and subgiant stars. This unfortunately excluded such potentially interesting targets as HD 19445 and HD 140283, bright stars whose higher effective temperatures produce much larger relative *UV* fluxes than giants do. Our attention was thus focused on choosing the best metal-poor giants for observation.

We gathered data in four near-*UV* spectral regions of HD 122563 and three regions in the other two stars. The spectral regions were selected to contain low excitation transitions of 3rd-peak species Os I, Pt I, Ir I, and Pb I. We will justify the wavelength settings of the GHRS integrations in §3; here we comment on the program stars.

HD 122563 was chosen for HST Cycle 4 observations simply because it is by far the brightest very metal-poor star ([Fe/H] ~ -2.7) in the sky. This star has long been known (Wallerstein *et al.* 1963) to have relative underabundances of the rare earth elements (*e.g.*, [Eu/Fe] $\simeq -0.4$; Sneden & Parthasarathy 1983, Gratton & Sneden 1994, and references therein). Thus we expected very weak *UV* lines of the neutron-capture elements in this star. During HST Cycle 5, we obtained GHRS spectra in three wavelength regions of HD 126238. The number of wavelength regions was reduced to keep the requested total GHRS exposure time reasonable, because HD 126238 is a magnitude fainter than HD 122563. This star is moderately metal-poor ([Fe/H] ~ -1.7; Gratton & Sneden 1991) and has relative neutron-capture element abundances similar to solar-system values (*i.e.*, [n-capture/Fe] ~ 0; Gratton & Sneden 1994). Our expectations of strong *UV* lines of 3rd-peak elements were confirmed by the GHRS spectra (Cowan *et al.* 1996). Finally, we observed three wavelength regions of HD 115444 during Cycle 6. This star has a similar metallicity ([Fe/H] ~ -2.8) to HD 122563, but its rare-earth elements are much more abundant (*e.g.*, [Eu/Fe] $\simeq +0.4$; Griffin *et al.* 1982, Gilroy *et al.* 1988). Therefore HD 115444 is of special interest, even though it is nearly three magnitudes fainter than HD 122563, thus requiring either longer exposures or a sacrifice of S/N in the spectra.

The GHRS operating characteristics have been discussed extensively by Gilliland *et al.* (1992). For our observations the spectrograph was configured with the low-order grating G270 and the "small science" entrance aperture. We employed a sub-stepping pattern of four slightly shifted grating positions per detector diode for each observation. The spectra each spanned wavelength ranges of approximately 45 Å, and had central wavelengths near $\lambda\lambda$2830, 2915, 3060, and (only for HD 122563) 3010 Å. The resolving power of each reduced spectrum was R $\simeq$ 32,000 as determined by inspection of calibration lamp spectra, and the S/N was between 50 and 70.

We employed IRAF software for the first parts of the spectrum reductions, following standard recipes in the "HST Data Handbook" (Baum 1994). In this manner, we aligned the sub-stepped integration parts in wavelength, co-added the spectra, attached the wavelength scales, and wrote FITS images of the spectra. Final reductions, using the SPECTRE spectrum analysis package

(Fitzpatrick & Sneden 1987), involved continuum normalization, elision over a few bad pixels, and spectral feature identification. We also implemented in SPECTRE the spectrum de-convolution algorithm recommended by Gilliland *et al.* (1992) in order to recover the higher spectral resolution inherent in the original sub-stepped integration pattern. The de-convolution was used to be sure of the identification of a few blended features, especially the λ3064 Å line of Pt I (see §3.1).

3. The Neutron-Capture Elements: Solar Studies and Transitions in the GHRS Spectra

The *UV* spectra of even very metal-poor stars are complex, and line identification requires careful assessment of atomic and molecular (mainly OH) contaminants to the features of interest. With the aid of a variety of published line lists, we selected neutron-capture species features to be observed (concentrating on 3rd-peak element transitions) and then identified those features in the reduced GHRS spectra. General sources included: a) the solar spectrum identifications of Moore *et al.* (1962) and especially Moore *et al.* (1982); b) the voluminous atomic and molecular line lists of R. L. Kurucz (described in Kurucz 1995a,b), which are expansions of the "semi-empirical gf" tables of Kurucz & Peytremann (1975); c) the compilations of atomic transitions by the NBS (now NIST) group (*e.g.*, Reader & Corliss 1980); d) the original large-scale laboratory transition probability study of Corliss & Bozman (1962); and e) the on-going NIST "critical compilation" of the most reliable gf values. A discussion of the NIST compilation has been given by Wiese *et al.* (1995), and for a current version of their work see Fuhr & Wiese (1996).

For base-line abundances we adopted the solar photospheric and solar system meteoritic abundances recommended by Grevesse *et al.* (1996; hereafter called GNS96); we will comment below on specific cases. For the elements considered here, the GNS96 abundances do not differ substantially from those recommended in earlier solar abundance summaries (Grevesse 1984, Anders & Ebihara 1982).

The search for neutron-capture transitions was limited to the near-*UV* spectral region, defined here to be approximately the wavelength range 2700 Å $\leq \lambda \leq$ 3300 Å. The long wavelength limit was set by assuming that ground-based facilities could be used to observe features longward of this wavelength. The short wavelength limit was imposed by the rapidly decreasing fluxes of cool giant stars toward smaller wavelengths. In practice, the search for 3rd-peak elements became limited to neutral-species transitions that both arise from low excitation potential (E.P.) states and have large transition probabilities (log gf). The 3rd-peak elements have large first ionization potentials ($<$I.P.$> \sim 8.5$ eV, compared with $<$I.P.$> < 6.0$ eV for the rare earth elements near the 2nd-peak), and thus retain substantial neutral species populations even in giant stars. Ultimately, we identified transitions of 3rd-peak element species Os I (Z = 76), Pt I (Z = 78), and Pb I (Z = 82); 1st-peak species Zr II (Z = 40); and Ge I (Z = 32), which is a transition element in between the Fe-group and 1st-peak elements. Since four of these five detected elements are rarely studied in cool stars, for the remainder of this section we discuss the specific transitions that we observed for each species, and comment on its solar photospheric abundance. Attention will be drawn especially to the comparison between HD 122563 and HD 115444, since they are so similar in atmospheric parameters and metallicity.

3.1. Platinum

There are several Pt I lines in the near-UV that have favorable (E.P., log gf) combinations. Accurate lifetimes (Ramanujam & Andersen 1978) and branching ratios (Gough *et al.* 1982) exist for all of these lines: λ2929.79 Å (E.P. = 0.00 eV, log gf = −0.80); λ2997.97 Å (0.10 eV, −0.57); λ3064.71 Å (0.00 eV, −0.34); and λ3301.90 Å (0.81 eV, −0.89). Burger & Aller (1975) originally determined the solar platinum abundance from the latter three lines. Youssef & Khalil (1987) used updated atomic data to reconsider just the λ3301 Å line. Their derived value of log ϵ(Pt) = 1.74 is close to the photospheric and meteoritic values recommended by GNS96 (1.8 $\pm$ 0.3 and 1.69 $\pm$ 0.04, respectively), although GNS96 clearly do not consider the photospheric abundance to be well determined.

The λ3301 Å Pt I line is severely blended in the Sun (see Figure 1 of Youssef & Khalil 1987). Moreover, since it has the highest E.P. and lowest log gf among the quartet of possible Pt I lines, it will definitely be the weakest of them in cool giant star spectra. We therefore discarded the λ3301 Å line and observed the other three lines in HD 122563. Initial attempts to match synthetic spectra with the observed λ2997.97 Å line in this star showed that the blending from an OH line at λ2998.01 Å was too severe to yield a useful abundance or upper limit, so this line also was discarded. We did not repeat observations of the λ2997 Å line in HD 126238 and HD 115444, even though the Pt I contribution would probably have been detectable over the OH contamination in these stars.

The observed spectra of the remaining two candidate Pt I lines are shown in Figure 1. The same plotting conventions are used in Figures 1–4; see Figure 1's caption for details. We emphasize here that for these four figures, small downward vertical shifts have been introduced to the spectra of HD 115444 and HD 126238, in order to separate them from each other and from HD 122563 near the spectrum continuum level. Therefore although most absorption features in HD 115444 seem to have similar depths to those of HD 122563 in these figures, they are actually weaker when the continua are normalized consistently. This is understandable since these two stars have similar *but not identical* atmospheric parameters: HD 115444 is somewhat hotter, has a larger gravity, and may be slightly more metal-poor than HD 122563. All of these parameter differences lead to a somewhat weaker line spectrum on average for HD 115444 compared to HD 122563.

The λ2929.79 Å Pt I line (Figure 1, left-hand panel) cannot be detected with any certainty in HD 122563. This statement holds in general for all 3$^{\rm rd}$-peak neutron-capture species lines in HD 122563 that will be discussed below. On the other hand, the λ2929 Å line is quite strong in HD 115444. The contrast in Pt I line strengths is made sharper by the slight weakness of most

HD 115444 lines compared with those of HD 122563 that we noted above. The λ2929 Å line also is strong in HD 126238, but so are all other features in this star, since it is about 10 times less metal-poor than the other two stars.

The λ3064 Å lines are displayed in the right-hand panel of Figure 1. This line ought to be the strongest of all Pt I lines, but frustratingly it lies in a clump of very strong atomic and OH lines. It suffers most contamination from a deep Ni I line at λ3064.62 Å. However all is not lost here, as close inspection of the reduced spectra reveals that the total Ni+Pt blend is not the same in HD 122563 and HD 115444: the latter star's feature has a redder central wavelength caused by an obvious extra absorption component in the red wing of the feature. Pt I contributes substantially to the feature strength in HD 115444 but cannot be identified with certainty in HD 122563. The extra line breadth due to two component contributions to the feature is even more obvious in HD 126238. For this blend, we applied the Gilliland *et al.* (1982) de-convolution algorithm to recover higher resolution spectra for the three stars, and the de-convolved spectra are the ones chosen for Figure 1's right-hand panel. Of course, the price paid for de-convolution is lower S/N, and this is apparent in the λ3064 Å spectra here. However, the presence (or absence) of the Pt I contribution is made much more apparent with this technique.

3.2. Osmium

Many Os I transitions are scattered throughout the UV and visible spectral regions, allowing a reliable solar photospheric osmium abundance to be determined. The first such study was by Jacoby & Aller (1976). A more recent analysis by Kwiatkowski *et al.* (1984) yielded $\log \epsilon(\mathrm{Os}) = 1.45 \pm 0.10$. This has been adopted as the standard value by GNS96, and is in good agreement with their recommended meteoritic abundance of 1.37 ± 0.02.

Unfortunately, the (E.P., log gf) combinations of all Os I transitions longward of λ3400 Å render all solar and stellar lines of this species quite weak. To our knowledge, only the Sneden *et al.* (1996) analysis of the very neutron-capture-rich halo giant CS 22892-052 included an osmium abundance for a metal-poor star, and their reported [Os/Fe] value was quite uncertain. The predicted strengths of these "long wavelength" Os I lines were vanishingly small for our program stars, so we turned attention to the near-UV transitions.

Accurate transition probabilities of some of these lines have been determined by Kwiatkowski *et al.* (1984). For other lines, the values of Corliss & Bozmann (1962) can be reliably scaled to the system defined by Kwiatkowski *et al.*'s lifetime measurements. Candidate Os I lines initially considered for observations were: λ2838.63 Å (E.P. = 0.64 eV, log gf = +0.11); λ2909.06 Å (0.00 eV, −0.32); λ3058.66 Å (0.00 eV, −0.43); and λ3301.58 Å (0.00 eV, −0.75). The λ2909 Å line is unfortunately unusable, as it is masked by a strong Cr I line at λ2909.04 Å. The λ3301 Å line is more promising, even though it lies close to a fairly strong Ti I line (λ3301.68 Å). This line was used in Kwiatkowski *et al.*'s solar abundance study, but we did not consider it highest priority for

GHRS observations. It could be better observed in our stars using large ground-based telescopes and good near-UV spectrograph–detector combinations.

We obtained GHRS spectra of the remaining two Os I lines; these are displayed in Figure 2. For HD 115444, the S/N is highest for the "3060 Å" spectrum because by happy accident the total GHRS exposure time for this spectrum was three times longer than requested. This is apparent when comparing this star's Os I lines at λ2838.63 Å (left-hand panel, Figure 2) with its λ3058.66 Å line (right-hand panel). However, the lower S/N of the HD 115444 "2830 Å" spectrum does not obscure the contrast with HD 122563: Os I lines, just like Pt I lines, are weak-to-absent in HD 122563, but easily detectable in HD 115444. Note that the λ3058 Å line suffers some blending with an Fe I line that lies 0.05 Å redward of it. The blending agent is undetectably weak in the very metal-poor HD 122563 and HD 115444, but does influence the total strength of the Os I feature in HD 126238. The derived Os abundance from this line in HD 126238 should be viewed with caution.

3.3. Zirconium

This element lies near the 1st neutron-capture peak, and Zr II presents a rich spectrum of strong lines in cool stars. Biémont *et al.* (1981) performed an extensive laboratory study of Zr II transition probabilities, and their comparison solar abundance analysis yielded log ϵ(Zr) = 2.60 $\pm$ 0.02, which is almost exactly the meteoritic value of 2.61 $\pm$ 0.02 (GNS96). Zirconium is of special interest here because the previously cited analyses of our program stars have all reported abundances of this element. Thus similar analyses of Zr II lines appearing on our GHRS spectra should provide reliability checks on our procedures for elements that are being studied here for the first time.

Of the possible Zr II near-UV transitions, the two most useful features proved to be those displayed in Figure 3: λ3054.84 Å (E.P. = 1.01 eV, log gf = +0.18) and λ3060.11 Å (0.04 eV, –1.37). Unlike the sharp differences in the Pt I and Os I lines between HD 122563 and HD 115444, the Zr II lines of these two stars have nearly identical strengths, suggesting of course that their zirconium abundances are very similar. In §4, we confirm this impression and in §5 we argue that the ground-based zirconium abundance derivations are in good agreement with our conclusion.

3.4. Lead

This element is the next-to-heaviest stable element in the periodic table. It is synthesized in both r- and s-process neutron capture syntheses, and it is the fission decay product of heavier unstable elements such as thorium and uranium. The solar photospheric lead abundance has been determined in several investigations, most recently by Youssef & Khalil (1989); see their paper for references to early studies. Their photospheric abundance, log ϵ(Pb) = 2.00 $\pm$ 0.05, is in reasonable agreement with the meteoritic value of 2.06 $\pm$ 0.04 recommended by GNS96.

However, both of these abundances may need revision. Grevesse & Noels (1993) recalculated the photospheric abundance from Youssef & Khalil's data and obtained log ϵ(Pb) = 1.95 ± 0.08, and that value has been adopted by GNS96.

The largest challenge for solar and stellar lead abundance analyses is that the four accessible Pb I lines in the visible spectral region are weak and lie in crowded spectral regions; line blending problems are severe. None of these Pb I lines has a favorable enough (E.P., log gf) combination to ensure detectability in metal-poor stars. Sneden *et al.* (1996) searched without success for the λ3683.48 Å (0.97 eV, −0.60) and λ4057.82 Å (1.32 eV, −0.20) lines in the spectrum of CS 22892-052.

Pb I has only one transition in the near-UV that predicts reasonable absorption strength from its atomic parameters: λ2833.05 Å (0.00 eV, −0.68). Happily, this line lies close enough to the λ2838 Å Os I line that one GHRS integration could capture them both. The left-hand panel of Figure 4 displays a now-familiar story: non-detection in HD 122563 and a very strong feature in HD 126238. The low S/N of our HD 115444 "2830" spectrum creates some difficulty here. We believe that the absorption feature slightly redward-displaced of the expected Pb I line position is indeed that line, but we recognize that this feature is quite narrow for a stellar absorption line, and is probably afflicted by some noise spike in its blue wing. Clearly we recommend caution in interpreting the lead abundance derived in §4 for HD 115444, and recommend re-observing this line in the future.

3.5. Germanium

An unexpected bonus was the detection of a strong Ge I line at λ3039.07 Å in our spectra. This feature is shown in the right-hand panel of Figure 4. Note the similarity of Ge I absorption strengths in HD 115444 and HD 122563. Germanium, with an atomic number Z = 32, is just beyond the iron-peak element group, thus occurring well below the 1st neutron-capture peak. With no strong transitions in the visible spectral range, this element has been neglected in stellar abundance studies and thus in nucleosynthesis discussions.

Transition probabilities for low-excitation Ge I lines have been determined several times (*e.g.*, Andersen *et al.* 1975, Lotrian *et al.* 1978, Tint *et al.* 1990, and references therein), and the gf uncertainties are small. Unfortunately, good atomic data have not led to satisfactory photospheric/meteoritic solar abundance agreement. GNS96 recommend log ϵ(Ge) = 3.41 ± 0.14 for the photospheric abundance (from Grevesse & Meyer 1985), and 3.63 ± 0.04 for the meteoritic value. Clearly they suspect that the 0.22 dex difference in these values is mostly the fault in the photospheric abundance. Apparently there are only two detectable Ge I lines in the visible region of the solar spectrum: $\lambda\lambda$4226.57,4685.85 Å. Both of these lines arise from higher excitation states (2.0 eV), and suffer from intrinsically weak absorption strengths compounded by severe contamination problems from other species; for detailed discussions of the λ4685 Å line see Lambert *et al.* (1969) and Grevesse & Meyer.

The λ3039 Å line has a well determined gf (Fuhr & Wiese 1996), and it has been a participant in solar abundance studies (Ross & Aller 1974), and it appears to be fairly clean in our metal-poor star spectra (Figure 4). Therefore the "absolute" log ϵ(Ge) abundances deduced from this line should be as reliable as those determined for other species in our study. However, relative [Ge/Fe] abundances will have larger uncertainties due to remaining questions about the solar germanium abundance.

3.6. Non-Observed 3rd-Peak Neutron-Capture Elements

Iridium, gold, mercury, and thallium complete the 3rd neutron-capture peak element domain ($76 \leq Z \leq 82$). No Tl I lines in our spectral region are identified in the solar spectrum (Moore *et al.* 1982); they should all be very weak, as the ionization potential of this species is only 6.1 eV. The resonance lines of Hg I (λ2536.52 Å) and Au I ($\lambda\lambda$2427.95,2675.95 Å) might be detectable in our stars, but they lie too far in the *UV* to be practical targets in this investigation. Higher excitation lines of these species are predicted to be undetectable. Several Ir I lines have provided a trustworthy photospheric abundance (Youssef & Khalil 1988), which is in excellent agreement with the meteoritic value recommended by GNS96. Neglecting the weak higher excitation lines, there are two promising transitions of this species: $\lambda\lambda$3220.78,2924.79 Å. Unfortunately, the λ3220 Å line at our spectral resolution would be too blended with an Fe II line at λ3220.84 Å to be of use in this study. The λ2924 Å line was searched for on our spectra, but test syntheses convinced us that this feature would be just a very small extra absorption in the red wing of a strong blend of Fe I and V II lines. Indeed, the Ir I strength compared to its contaminants would be much smaller than the strength of the Pt I λ3064 Å blended line that was discussed in §3.1. Therefore, not having the luxury of any additional Ir I lines on our spectra, this element was dropped from consideration.

4. Abundance Analysis

We determined abundances of the neutron-capture elements through matching synthetic and observed spectra for the program stars. In Table 1 we list the stellar model atmosphere parameters and the derived abundances.

The current version of the LTE line analysis program MOOG (Sneden 1973) was employed for the spectrum computations. Model stellar atmospheres were generated with the MARCS code (Gustafsson *et al.* 1975). For HD 122563 and HD 115444 we used model effective temperature T_{eff}, gravitation acceleration log g, model metallicity [M/H], and microturbulent velocity v_t from Pilachowski *et al.* (1996), and for HD 126238 we adopted the parameters of Gratton & Sneden (1991,1994). These are listed in the top section of Table 1, along with the [Fe/H] values derived in the cited studies. The T_{eff}, log g, and [M/H] parameters served as input data to the MARCS code.

We then created an input line list for each synthetic spectrum computation. First we assembled an initial list of atomic and OH molecular lines from the Kurucz (1995a,b) compilation for a wavelength range of several Å centered on a neutron-capture feature of interest. To increase computation speed, we discarded lines from this list that contribute essentially nothing to the total line opacity in cool stars, such as multiply ionized species lines, or ones that have excitation potentials in excess of $\sim$ 6 eV. We added a few lines that were identified in the Moore *et al.* (1962,1982) solar spectrum atlases but are missing from the Kurucz compilation.

Initial synthetic spectra generated with these line lists and the model atmospheres for our stars yielded only fair matches with observed spectra. However, we have repeatedly noted in §3 that a) many neutron-capture species lines (all of the 3^{rd}-peak ones) cannot be detected on the GHRS spectra of HD 122563 but are quite strong in HD 115444, and b) in all other respects the spectra of HD 122563 and HD 115444 are quite similar. Taking advantage of this situation, we empirically iterated on the transition probabilities of lines in the synthetic spectrum lists until a reasonable match was made to the observed HD 122563 spectrum, and then applied those line lists to the other stars. A few rules constrained this game. First, the gf values for the neutron-capture transitions under scrutiny were frozen; all of these have undergone recent laboratory studies (see the discussion in §3). Second, the gf values of individual OH lines were not altered except in rare cases in which OH lines were predicted to exist at locations where little absorption is present in the observed spectra. Instead, the strengths of all OH lines were changed together by altering the assumed oxygen abundance (assumed to be a free parameter here) in the synthetic spectrum computations. Third, for HD 122563 the initially assumed abundances of 3^{rd}-peak elements osmium, platinum, and lead were extrapolated from the low levels of its previously-determined (*e.g.*, Sneden & Parthasarathy 1983, Gratton & Sneden 1994) rare-earth neutron-capture abundances. This assumption essentially guaranteed that the line opacities of these species would be quite small in HD 122563, and that any residual absorption observed at their wavelengths in HD 122563 could be used to set upper limits to the feature contamination from other species.

For all three program stars, synthetic spectra with the final line lists were generated for several different assumed abundances of the neutron-capture species, holding all other abundances constant at the values derived in previous ground-based studies. The "absolute" log ϵ abundance derived from each synthetic/observed spectrum match is given in the second section of Table 1. The upper limits quoted in Table 1 for HD 122563 were estimated through experimental synthetic spectrum computations in which we muted the blending agents to the neutron-capture species lines, leaving any observed absorption to be blamed on the neutron-capture lines alone. In Figures 5 and 6 we display samples of the synthetic/observed spectrum matches. Notice especially that the "goodness of fit" for features other than the neutron-capture species features is about the same for HD 122563 and HD 115444. There are sections of observed spectra in which there are inadequacies in the synthetic spectra; for example, in Figure 5 there is an unidentified absorption near λ2929.2 Å. However, that feature appears in all three spectra, so we have some confidence in applying the HD 122563 iterated line list to HD 115444. The extrapolation to HD 126238, a factor of 10 higher in metallicity, is not quite as good. For example, the synthetic spectra predict deeper features near λ2929.4 Å than are actually observed (Figure 5), and an absorption due to Co I λ3050.05 Å is too strong in the synthetic spectra of HD 126238 (Figure 6), making it very difficult to derive a zirconium abundance from the Zr II λ3060.11 Å line in this star. Happily, such cases are rare in the features considered in this study.

Uncertainties in derived abundances due to stellar atmospheric parameter uncertainties for typical lines of this work have been considered at length in other publications (*e.g.*, §3.5 in Sneden *et al.* 1996), and will not be repeated here. The total abundance uncertainty due to these errors is about $\pm$ 0.10 dex. Uncertainties in the synthetic/observed spectrum matches contributes another $\pm$ 0.15 dex. The solar abundances of all but germanium appear to be well determined, and so are the transition probabilities of all lines analyzed here, and we estimate that these uncertainties add another $\pm$ 0.10 dex to the derived abundances. We estimate that taking all these error sources into account, the total uncertainty in the neutron-capture abundances $\pm$ 0.25 dex.

One potentially troublesome analysis uncertainty should be addressed here. For most stellar abundance work, model atmospheres are generated with the MARCS code or the ATLAS code of Kurucz (1970). These programs employ standard assumptions such as LTE and plane-parallel geometry, and account for atomic and molecular line opacities with opacity distribution functions. These assumptions yield reasonable results for most stars, but there are persistent concerns that predicted stellar fluxes may be substantially larger than observed ones in *UV* spectral regions. This problem is assumed to be due to "missing opacities", probably from uncataloged atomic and molecular transitions in the *UV*. For a general discussion of this question, see *e.g.* Buser & Kurucz (1992), and references therein. However, for extremely metal-poor stars the atomic line opacities are sharply reduced, and for our program star HD 122563 the *UV* flux question has already been addressed by Gustafsson *et al.* (1980). They showed that theoretical fluxes from MARCS models agree well with IUE spectral fluxes in the wavelength range 2300 Å $\leq \lambda \leq$ 2650 Å (the longer wavelength IUE flux points were saturated, thus not very useful for the comparison with model fluxes). Therefore we expect the MARCS models to give reasonable fluxes in the 2830 Å $\leq \lambda \leq$ 3065 Å wavelength range of interest here, and that the missing *UV* opacity problem is not a large concern for our stars.

5. Discussion and Conclusions

The chief aim of this program has been to determine the abundances for some of the heaviest stable elements in very metal-poor stars. New HST observations of HD 115444 ([Fe/H] $\simeq$ –2.8) indicate the presence of the very heavy elements osmium, platinum, and lead. Adding to our earlier observations of the less metal-poor ([Fe/H] $\simeq$ –1.7) giant star HD 126238 (Cowan *et al.* 1996), this marks only the second detection of 3$^{\rm rd}$ neutron-capture peak elements in Galactic halo stars. (The element Os was detected by Sneden *et al.* (1996) in the star CS 22892–052, but with large uncertainties in the abundance.) Observations have also been made of HD 122563, which has a metallicity similar to that of HD 115444. However, in contrast to HD 115444, HD 122563 has a depressed level of heavy neutron-capture elements ($Z \geq 56$) and our HST observations failed to detect any of these elements in this star. The differences in 3^{rd}-peak abundances between these two stars was demonstrated qualitatively through the observed spectra (§3), and quantitatively via synthetic spectrum abundance computations (§4). We further noted the strong near-*UV* spectral lines of HD 126238, and the larger 3^{rd}-peak abundances consistent with that star's higher metallicity.

In this section we combine the available abundance data for neutron-capture elements for each star, compare these data to scaled solar-system abundance distributions, and relate this information to early Galactic nucleosynthesis. The basic abundance results are given in the third section of Table 1; these are straight means of the results from individual lines of each species. In the final section of the table, the abundances have been translated into [el/Fe] ratios, rounding the entries to the nearest 0.05 dex. These numbers will not be used in our nucleosynthesis discussion, but they serve to summarize the observational results: a) germanium abundances are quite low in all three stars; b) zirconium abundances are similar in HD 122563 and HD 115444; and c) most importantly, there is at least a 0.7 dex difference in the abundance level of 3^{rd} neutron-capture peak abundances between these two stars.

5.1. Stellar Abundances: Comparison with Solar Element Distributions

Consider first the very metal-poor star HD 115444. We have added ground-based data (open circles) to our HST abundances (filled circles) for this star (see Figure 7). The ground-based abundances are straight means of those reported in the two published abundance studies of this star (Griffin *et al.* 1982; Gilroy *et al.* 1988). The error bars for the ground-based abundance results were estimated from the scatter in the individual abundance estimates of these two studies. Abundances for only nine neutron-capture elements have been reported for HD 115444; further work with better data clearly are needed. However, there is very pleasing agreement between the ground-based and GHRS near-*UV* abundances for zirconium; this suggests that our abundance scale is in reasonable accord with ground-based studies of this star.

We have added to Figure 7 scaled solar-system abundance distributions for the total elemental abundances $\log \epsilon_\odot$ and *r*-process fractional abundances $\log \epsilon_\odot F_\odot[r]$. The total solar system elemental abundances are from the compilations of Anders & Ebihara (1982) and Anders & Grevesse (1989), and are indicated in this figure by a dashed line. We de-convolved the elemental abundances into *r*- and *s*-process contributions, computing the *r*-process fraction $F_\odot[r]$ for each element using the work of Käppeler *et al.* (1989), with some recent selected additions from Wisshak *et al.* (1996). This de-convolution process is discussed more fully by Sneden *et al.* (1996) and Burris *et al.* (1997). The scaled *r*-process curve is illustrated in Figure 7 as a solid line. Both of these solar curves have been displaced downward by a single-valued additive constant, to compensate for the lower metallicities of these stars. The vertical normalization of the solar curves in Figure 7 was chosen to match the observed samarium (76% solar *r*-process) and europium (97% *r*-process) abundances. But this normalization simultaneously also yields good fits to the *r*-process solar fractional curve for the 3rd neutron-capture peak elements osmium and platinum, and the much lighter elements yttrium and zirconium. Outliers are cerium (we suspect that a new HD 115444 analysis will decrease this abundance), germanium (below the solar-system curves in all three stars), and zirconium (perhaps there is an *s*-process component to this abundance). We also remind the reader that for lead, in spite of the apparent good agreement between observed and *r*-process predicted abundances, the stellar value is quite uncertain. While it is possible to argue about the fit for individual elements, the overall agreement between the solar system *r*-process curve and the elemental abundances in HD 115444 is very compelling. With the new HST observations of this star, however, we have a wider range of elemental abundances (from Ge through Pt) than ever before possible.

We have made a similar abundance comparison for the well-studied halo star HD 122563. In Figure 8 we plot (with open circles) the abundances for 14 neutron-capture elements determined from ground-based spectra. So many abundance analyses have been published for this star (and all in reasonable accord with each other) that we have chosen to plot abundances that are means of those deduced by Wolffram (1972), Spite & Spite (1978), Sneden & Parthasarathy (1983), Gilroy *et al.* (1988), Peterson *et al.* (1990), Gratton & Sneden (1994), and Ryan *et al.* (1996). Double weight was assigned to the abundances of Gratton & Sneden, since their observational data were probably the best and they reconsidered solar abundances as well as stellar ones in their analysis.

In Figure 8 we also plot (with filled circles) abundances or upper limits for the five neutron-capture elements considered in the present study. The zirconium abundance determined from GHRS near-UV data (log ϵ(Zr) $\simeq$ +0.22) is somewhat larger than the mean of the ground-based abundances (log ϵ(Zr) $\simeq$ +0.01), but the agreement is within the error bars. This suggests that our abundance might not have significant scale errors, at least for HD 122563. The vertical normalization was set to produce the best average agreement between the solar distributions and that of the elemental abundances of europium, gadolinium and dysprosium in HD 122563, since these elements are nearly pure *r*-process ones in solar-system material.

As has been pointed out in several of the cited papers, nearly all HD 122563 abundances in the range $56 \leq Z \leq 70$ are well fit by the scaled *r*-process solar-system distribution. Cerium may be an exception, but we note that its observed abundance would have been $\sim$ 0.2 dex smaller if we had used just the Gratton & Sneden (1994) abundance. Contributions of the *s*-process to the observed abundances must have been quite small from the progenitor to this star. Our osmium, platinum, and lead upper limits are not inconsistent with either the scaled solar *r*-process or the solar total distribution. But these upper limits yield little useful information on the 3rd neutron-capture peak abundances in HD 122563. A comparison of Figures 8 and 7 re-emphasizes that the absolute abundance levels of elements throughout the range $56 \leq Z \leq 82$ in HD 115444 are nearly an order-of-magnitude greater than those in HD 122563, even though both stars have the same iron abundance.

The final abundance comparison, this time for the less metal-poor HD 126238, is shown in Figure 9. The ground-based data of Gratton & Sneden (1994) have been added to our HST abundances for this star. The stellar neutron-capture abundances in the range $60 \leq Z \leq 82$ match well the scaled solar r-process distribution, while many of the lighter neutron-capture elements show evidence for some s-process contribution. The total abundance level of the neutron-capture elements in this star is somewhat higher than in HD 115444. However, the ratio of the 3rd-peak element abundances to that of the pure r-process element europium is *the same in both stars*: $\log \epsilon = 1.35 \pm 0.1$. These new abundances, along with the ground-based data of CS 22892-052 (Sneden *et al.* 1996) are remarkably consistent. The abundances of most neutron-capture elements beginning with the rare-earths, and all the way out to the 3rd-peak elements have relative solar r-process ratios. This agreement is now seen in stars of different metallicities, with a wide range of elements running through the most massive stable elements, and with stars of very different absolute abundance levels of neutron-capture elements. The total neutron-capture element distributions for $Z > 55$ in these stars (and others) strongly suggest that the basic mechanism of r-process nucleosynthesis for 2nd and 3rd-peak elements has not changed significantly over the history of the Galaxy, and thus, that the solar system r-process abundances for these elements could not be the average of r-process products from a number of different environments (see also Cowan *et al.* 1995, 1996, 1997a). These extensive new results also make less plausible other explanations for these stellar abundance ratios, for example individual nuclear or random effects (see *e.g.* Goriely & Arnould 1997).

5.2. A Second r-Process?

The behavior of the lighter neutron-capture elements depicted in Figures 7–9, does not seem to follow the solar r-process curve as clearly as the heavier elements. We see for example that strontium and yttrium lie close to the solar r-process curve for HD 115444, but zirconium is significantly above it. In HD 122563 all three of these elements lie appreciably above the r-process curve, with zirconium well above the *total* scaled solar abundance curve. Thus, these two stars with the same overall metallicity have very different abundance levels for both the light and heavy neutron capture elements. The critical difference is that the lighter neutron-capture elements in both stars do not follow the solar r-process ratios, in contrast to those elements above $Z = 55$. The same apparent disjunction between the light and heavy neutron-capture elements is seen in the more metal-rich HD 126238, where yttrium lies on the scaled solar r-process curve but strontium and zirconium are overabundant. These three elements are near each other in nuclear mass, and the observed relative abundance pattern is similar in all three stars. This would suggest that Sr–Y–Zr are produced together in a similar environment, but the situation is unclear at this point.

We also note that newly detected germanium does not follow the scaled solar curves in any of the three stars. This element is produced in approximately equal amounts by the r- and s-process in solar material (Sneden *et al.* 1996). Thus, naively it would be expected that the abundance of germanium in the old, metal-poor stars would be less than total solar (with little or no *s*-process contribution), but would scale with the solar *r*-process curve similarly to the heavier neutron-capture elements. But in all three program stars, germanium has a significantly subsolar abundance. Interestingly germanium, like zirconium, does seem to scale with metallicity in the three observed stars – it is identical in HD 115444 and HD 126238, but significantly greater in the higher metallicity HD 126238.

Our results appear to lend support to the suggestion that lighter neutron-capture elements may be produced in a different, or second *r*-process (Wasserburg *et al.* 1996). We refer the reader to, *e.g.*, Cowan *et al.* 1991 and Mathews *et al.* 1992 for a discussion of various possible *r*-process sites and environments. We caution, however, that there are too few data for these elements in the metal-poor stars, and other effects such as the weak component of the *s*-process, expected to occur during core helium burning in massive stars (see *e.g.*, Raiteri *et al.* 1993), may complicate the abundance interpretation for the elements of germanium and the Sr–Y–Zr group. To determine whether there are at least two different *r*-processes will require further examination of the abundance trends of the lighter neutron-capture elements, particularly those near mass number 100, just above the first *r*-process peak. Such observations, including those of the element Ag (A $\sim$ 108), are currently in progress (Crawford *et al.* 1997), but the target stars in that investigation do not include any with as low metallicities as HD 122563 or HD 115444. Additional calculations, such as those by Thielemann *et al.* (1997) exploring different synthesis environments, will also be necessary to ascertain if there are multiple conditions required for the total solar system *r*-process abundance distribution.

5.3. Galactic Chemical History

Our new HST observations and abundance comparisons provide insight into the early nucleosynthetic history of the Galaxy and the nature of the first stellar generations. The three metal-poor halo stars studied here, along with the ultra-metal-poor star CS 22892-052, must have been formed shortly after the beginning wave of Galactic element generation. Even though many of the neutron-capture elements are synthesized by a combination of the *r*- and *s*-processes in solar material, these metal-poor halo stars show mainly a scaled-down version of the solar system *r*-process only (for most elements with Z $\geq$ 56), confirming that contributions from the *r*-process dominated at the earliest stages of Galactic history. This result strengthens the use of chronometers, *e.g.*, the long-lived *r*-process element thorium, in estimating the age of the Galactic halo (*e.g.*, François *et al.* 1993, Sneden *et al.* 1996, Cowan *et al.* 1997a).

In addition, the presence of the *r*-process elements in the halo stars demonstrates the existence of previous stellar generations of *r*-process progenitors. This follows since the *r*-process elements are not likely produced during quiescent stellar evolution (Cowan *et al.* 1991), and thus their presence in these halo stars cannot be the result of self-contamination. Supernovae are considered likely sites for the *r*-process (Cowan *et al.* 1991 and references therein), although neutron-star binaries may also contribute or be a significant source (Mathews *et al.* 1992). If the time-lag between the formation of the Galaxy and the birth of the present halo stars was relatively short, the halo star progenitors and sites for the *r*-process must have evolved quickly. These results therefore suggest the presence of a generation (or generations) of massive stars, the progenitors of Type II supernovae, early in the history of the Galaxy (see also Cowan *et al.* 1995).

With only three stars studied here it is not possible to determine any definitive trends between halo metallicity and age. We note however that in the less metal-poor star HD 126238 there is some divergence from the *r*-process curve for the elements near barium (synthesized primarily via the *s*-process in solar system material). Cowan *et al.* (1996) suggested that this might indicate the onset of some Galactic *s*-processing. Figure 9 illustrates that the total solar curve is inconsistent with the Ba abundance. Instead this comparison suggests, as noted by Cowan *et al.* (1996), that perhaps only the more massive stellar sites for the *s*-process had time to evolve prior to the birth of HD 126238. These comparisons might suggest a (somewhat) longer time-scale between the birth of the Galaxy and HD 126238 and the other two stars studied here; HD 126238 might be (somewhat) younger. However, the data to support this conclusion are quite meager at this point. We further note the well-known problems associated with using the element barium in making these comparisons. Although it has been know for some time (Truran 1981) that the *r*-process contribution to barium production could be used to study the early synthesis history of the Galaxy, this element is overwhelmingly produced in the *s*-process — in fact, it dominates the second *s*-process peak seen in solar material. Nevertheless, since the elements tellurium (Z = 52) and xenon (Z = 54), which form the second *r*-process peak, are not detectable at this point in halo stars, barium must be employed as a tracer of both *r*- and *s*-process production for elements near the second n-capture peak. Observational and theoretical studies, using a number of elements including barium (Burris *et al.* 1997), are currently in progress in an attempt to determine the relationship between *r*- and *s*-process abundance contributions and large-scale halo parameters (age? metallicity? kinematics? evolutionary state?). These studies may also help in examining the conditions that occurred early in the Galaxy and its chemical evolution.

We thank James Crawford, Ron Gilliland, Inese Ivans, David Lambert, Craig Wheeler and George Wallerstein for helpful conversations, and we appreciate the expert help of the STScI staff in all aspects of the planning and execution of the observations over three HST Cycles. Support for this work was provided through grants GO-05421, GO-05856, and GO-06748 from the Space Science Telescope Institute, which is operated by the Association of Universities for Research in Astronomy, Inc., under NASA contract NAS5-26555. Support was also provided by the National Science Foundation through grants AST-9315068 and AST-9618364 to C.S., AST-9314936 and AST-9618332 to J.J.C, and AST-9217969 to J.W.T. This work was completed while C.S. was in residence at the University of Oklahoma, funded through the University of Texas as a Big XII Faculty Fellow; we are very grateful to both institutions for their support of this research. Revisions to this paper were completed when J.J.C. was in residence at the Institute for Theoretical Physics at the University of California Santa Barbara and supported in part by the

National Science Foundation under Grant No. PHY94-07194.

REFERENCES

Anders, E. & Ebihara, M. 1982, Geochim. Cosmochim. Acta, 46, 2363

Anders, E. & Grevesse, N. 1989, Geochim. Cosmochim. Acta, 53, 197

Andersen, T., Petkov, A. P., and Sorensen, G. 1975, Phys. Scr, 12, 283

Baum, S. 1994, HST Data Handbook, Sp. Tel. Sci. Inst., Baltimore

Biémont, E., Grevesse, N., Hannaford, P., & Lowe, R. M. 1981, ApJ, 248, 867.

Burger, H., & Aller, L. H. 1975, Proc. Nat. Acad. Sci. USA, 72, 4193

Burris, D. L., Pilachowski, C. A., Armandroff, T., Sneden, C., and Cowan, J. J. 1997, in preparation

Buser, R., & Kurucz, R. L. 1992, A&A, 264, 557

Corliss, C. H., & Bozman, W. R. 1962, Experimental Transition Probabilities for Spectral Lines of Seventy Elements, NBS Monograph 32, U. S. Government, Washington

Cowan, J. J., Burris, D. L., Sneden, C., McWilliam, A. & Preston, G. W. 1995, ApJ, 439, L51

Cowan, J.J., Sneden, C., Truran, J. W. & Burris, D. L. 1996, ApJ, 460, L115

Cowan, J.J., Thielemann, F.-K. & Truran, J.W. 1991, Phys. Rep., 208, 267

Cowan, J.J., McWilliam, A., Sneden, C. & Burris, D. L. 1997a, ApJ, 480, 246

Cowan, J. J., Sneden, C., Truran, J. W. & Burris, D. L. 1997b, in Proceedings of The Scientific Impact of the Goddard High Resolution Spectrograph, in press

Crawford, J., Sneden, C., King, J. R., Boesgaard, A. M., and Deliyannis, C. 1997, in preparation

Fitzpatrick, M. J., & Sneden, C. 1987, BAAS, 19, 1129

François, P., Spite, M., and Spite, F. 1993, A&A, 274, 821

Fuhr, J. R., & Wiese, W. L. 1996, NIST Atomic Transition Probability Tables, in CRC Handbook of Chemistry and Physics, ed. D. R. Lide, CRC Press, Boca Raton FL, 10-128

Gilliland, R. L., Morris, S. L., Weymann, R. J., Ebbets, D. C., & Linder, D. J. 1992, PASP, 104, 367

Gilroy, K. K., Sneden, C., Pilachowski, C. A. & Cowan, J. J. 1988, ApJ, 327, 298

Goriely, S. & Arnould, M. 1997, A&A, in press

Gough, D. S., Hannaford, P., & Lowe, R. M. 1982, J. Phys. B: At. Mol. Phys., 15, L431

Gratton, R., & Sneden, C. 1991, A&A, 241, 501

Gratton, R., & Sneden, C. 1994, A&A, 287, 927

Grevesse, N. 1984, Phys. Scr, T8, 49

Grevesse, N., and Meyer, J.-P. 1985, in Proc. 19th Cosmic Ray Conf., 3, 5

Grevesse, N, & Noels, A. 1993, in Origin and Evolution of the Elements, ed. N. Prantzos, E. Vangioni-Flam, & M. Cassé, Cambridge Univ. Press, 117

Grevesse, N, Noels, A., & Sauval, A. J. 1996, in Cosmic Abundances, PASP Conf. Ser. 99, ed. S. S. Holt and G. Sonneborn, 117

Griffin, R., Griffin, R., Gustafsson, B., and Vieira, T. 1982, MNRAS, 198, 637

Gustafsson, B., Bell, R. A., Ericksson, K., and Nordlund, A. 1975, A&A, 42, 407

Gustafsson, B., Bell, R. A., Fredga, K., and Gahm, G. F. 1980, A&A, 89, 225

Jacoby, G., & Aller, L. H. 1976, Proc. Nat. Acad. Sci. USA, 73, 1382

Käppeler, F., Beer, H. & Wisshak, K. 1989, Rep. Prog. Phys., 52, 945

Kurucz, R. L. 1970, SAO Spec. Rpt., No. 309

Kurucz, R. L. 1995a, in Astrophysical Applications of Powerful New Databases, PASP Conf. Ser. 78, ed. Adelman, S. J. & Wiese, W. L., 205.

Kurucz, R. L. 1995b, in Laboratory and Astronomical High Resolution Spectra, PASP Conf. Ser. 81, ed. Sauval, A. J., Blomme, R., & Grevesse, N., 583

Kurucz, R. L., & Peytremann, E. 1975, "A Table of Semiempirical gf Values", SAO Spec. Rpt. 362

Kwiatkowski, M., Zimmermann, P., Biémont, E., and Grevesse, N. 1984, A&A, 135, 59

Lambert, D. L., Mallia, E. A., and Warner, B. 1969, MNRAS, 142, 71

Lotrian, J., Cariou, J., Guern, Y., and Johannin-Gilles, A. 1978, J. Phys. B: Atom. Molec. Phys., 11, 2273

Mathews, G. J., Bazan, G. & Cowan, J. J. 1992, ApJ, 391, 719

McWilliam, A., Preston, G. W., Sneden, C., & Searle, L. 1995, AJ, 109, 2757.

Moore, C. E., Minnaert, M. G. J., & Houtgast, J. 1962, "The Solar Spectrum 2935Å to 8770Å", NBS Mono. 61

Moore, C. E., Tousey, R., and Brown, C. R. 1982, "The Solar Spectrum 3069Å to 2095Å", NRL Rep. 8653

Peterson, R. D., Kurucz, R. L., and Carney, B. W. 1990, ApJ, 350, 173

Pilachowski, C. A., Sneden, C., and Kraft, R. P., 1996, AJ, 111, 1689

Raiteri, C. M., Gallino, R., Busso, M., Neuberger, D. & Käppeler, F. 1993, ApJ, 419, 207

Ramanujam, P. S., & Andersen, T. 1978, ApJ, 226, 1171

Reader, J., & Corliss, C. H. 1980, Wavelengths and Transition Probabilities for Atoms and Atomic Ions. Part I. Wavelengths, NSRDS-NBS 68, U.S. Government, Washington

Ross, J. E., & Aller, L. H. 1974, Sol. Phys., 35, 281

Ryan, S. G., Norris, J. E., and Beers, T. C. 1990, ApJ, 471, 254

Sneden, C. 1973, ApJ, 184, 839

Sneden, C., & Parthasarathy, M. 1983, ApJ, 267, 757

Sneden, C., & Pilachowski, C.A. 1985, ApJ, 288, L55

Sneden, C., Preston, G. W., McWilliam, A. & Searle, L. 1994, ApJ, 431, L27

Sneden, C., McWilliam, A., Preston, G. W., Cowan, J. J., Burris, D. L. & Armosky, B. J. 1996, ApJ, 467, 819

Spite, M. & Spite, F. 1978, A&A, 67, 23

Thielemann, F.-K., Freiburghaus, C., Kolbe, E., Rauscher, T., Rembges, F., Kratz, K.-L., Pfeiffer, B., Schatz, H., Wiescher, M. & Cowan, J.J. 1997, in Proceedings of the 9th Capture Gamma-Ray Spectroscopy Symposium, ed. G. Molnar, (Budapest: Springer Hungarica) in press

Tint, K., Kono, A., and Goto, T. 1990, J. Quant. Spec. Rad. Trans., 43, 427

Truran, J. W. 1981, A&A, 97, 391

Wallerstein, G., Greenstein, J. L., Parker, R., Helfer, H. L, and Aller, L. H. 1963, ApJ, 137, 280

Wasserburg, G.J., Busso, M. & Gallino, R. 1996, ApJ, 466, L109

Wiese, W. L., Fuhr, J. R., Kelleher, D. E., Martin, W. C., Musgrove, A., and Sugar, J. 1995, in Astrophysical Applications of Powerful New Databases, ASP Conf. Ser. 78, ed. Adelman, S. J. & Wiese, W. L., 105

Wisshak, K., Voss, F. & Käppeler, F. 1996, in Proceedings of the 8^{th} Workshop on Nuclear Astrophysics, ed. W. Hillebrandt & E. Müller (Munich: MPI), 16

Wolffram, W. 1972, A&A, 17, 17

Youssef, N. H. & Khalil, N. M. 1987, A&A, 186, 333

Youssef, N. H. & Khalil, N. M. 1988, A&A, 203, 378

Youssef, N. H. & Khalil, N. M. 1989, A&A, 208, 271

Figure Captions:

Fig. 1.— GHRS spectra of the $\lambda\lambda$2929.79,3064.71 Å Pt I lines in HD 122563 ([Fe/H] = −2.7), HD 115444 ([Fe/H] = −2.7) and HD 126238 ([Fe/H] = −1.7). In Figures 1–4 the dotted lines always are used for HD 122563, solid lines for HD 115444, and dashed lines for HD 126238. All the spectra of these figures have been shifted in wavelength to align them in the rest-frame velocities of the stars. Also for display purposes, in these four figures we have shifted the spectra of HD 115444 and HD 126238 vertically downward in order to clearly separate the spectra of the three stars near their continuum regions. *In the right-hand panel of this figure only,* we show spectra that have been "de-convolved" according to the precepts of Gilliland et al. (1992) in order to increase spectra resolution and thus better uncover the λ3064.71 Å Pt I that is heavily blended with a λ3064.62 Å line of Ni I.

Fig. 2.— GHRS spectra of the $\lambda\lambda$2838.63,3058.66 Å Os I lines in the program stars. The plotting conventions are as in Figure 1.

Fig. 3.— GHRS spectra of the $\lambda\lambda$3054.84,3060.11 Å Zr II lines in the program stars. The plotting conventions are as in Figure 1.

Fig. 4.— GHRS spectra of the λ2833.05 Å Pb I and λ3039.07 Å Ge I lines in the program stars. The plotting conventions are as in Figure 1.

Fig. 5.— Observed spectra of the program stars (solid lines with points) compared with synthetic spectra (dashed lines) in the spectral region surrounding Pt I λ2929.8 Å. For HD 122563 (top panel), synthetic spectra have been generated for abundances log ϵ(Pt) = −1.90, −1.40, −0.90, −0.40; for HD 115444 (middle panel), log ϵ(Pt) = −1.00, −0.60 −0.20, +0.20; and for HD 126238 (bottom panel), log ϵ(Pt) = −0.85, −0.35, +0.15, +0.65.

Fig. 6.— Observed spectra of the program stars (solid lines with points) compared with synthetic spectra (dashed lines) in the spectral region surrounding Os I λ3058.7 Å and Zr II λ3060.1 Å. For HD 122563 (top panel), synthetic spectra have been generated for abundances log ϵ(Os) = −2.25, −1.75, −1.25, −0.75, and log ϵ(Zr) = −0.40, −0.10, +0.20, +0.50; for HD 115444 (middle panel), log ϵ(Os) = −1.80, −1.30, −0.80, −0.30, and log ϵ(Zr) = −0.45, −0.15, +0.15, +0.45; for HD 126238 (bottom panel), log ϵ(Os) = −1.20, −0.70, −0.20, +0.30, and log ϵ(Zr) = +0.65, +0.95, +1.25, +1.55.

Fig. 7.— An abundance comparison between the neutron-capture elements in HD 115444 and a scaled total solar system (dashed line) and solar system *r*-process (solid line) abundance distribution. Ground-based data (from various sources, see text for discussion) is indicated by open circles, while HST data is indicated by solid circles.

Fig. 8.— An abundance comparison for HD 122563 in the same style as that of Figure 7.

Fig. 9.— An abundance comparison for HD 126238 in the same style as that of Figure 7.

Table 1. Models and Abundances

Quantity	HD 122563	HD 115444	HD 126238
Stellar Model Atmosphere Parameters			
T_{eff} (K)	4625	4750	4975
log g	1.40	1.70	2.50
[M/H]	–3.00	–3.00	–1.65
v_t (km s^{-1})	2.0	1.6	1.5
logϵ Abundances from Individual Lines			
Ge I λ3039 Å	–0.10	–0.10	+1.15
Zr II λ3054 Å	+0.35	+0.05	···
Zr II λ3060 Å	+0.20	+0.25	···
Os I λ2838 Å	<–1.30	–0.40	+0.10
Os I λ3058 Å	<–1.30	–0.70	+0.20
Pt I λ2929 Å	<–1.30	–0.20	+0.50
Pt I λ3064 Å	<–1.20	–0.20	+0.60
Pb I λ2833 Å	<–0.80	–0.4:	0.00
logϵ Mean Abundances			
Ge	–0.10	–0.10	+1.15
Zr	+0.28	+0.15	···
Os	<–1.30	–0.55	+0.15
Pt	<–1.20	–0.20	+0.55
Pb	<–0.80	–0.4:	0.00
[el/Fe] mean Relative Abundances			
Ge	–3.50	–3.50	–1.25
Zr	–2.30	–2.45	···
Os	<–2.75	–1.85	–1.30
Pt	<–3.00	–2.00	–1.25
Pb	<–2.55	–2.25	–1.85

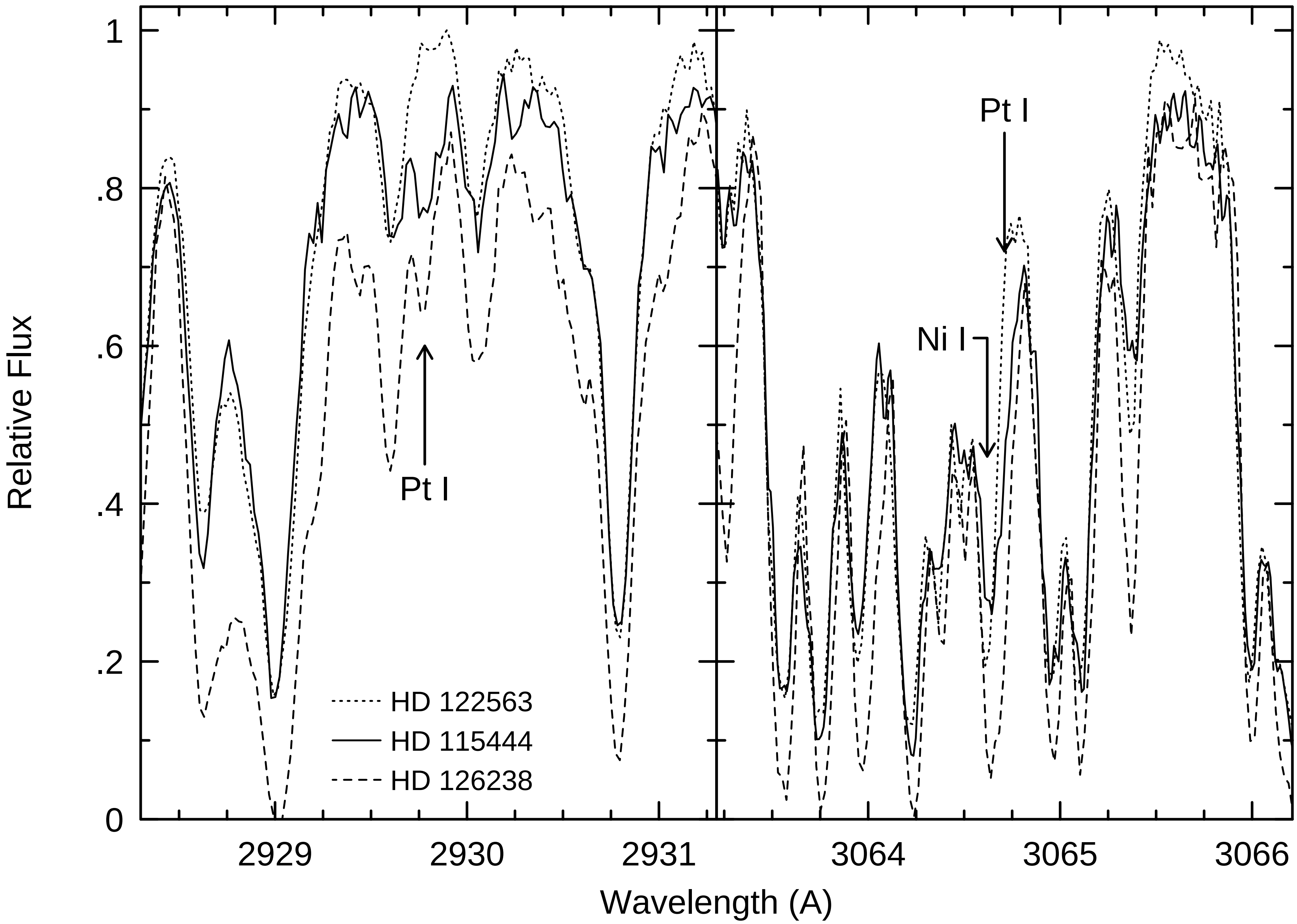

Relative Flux
1
.8
.6
.4
.2
0
2929
2930
2931
3064
3065
3066
Wavelength (A)
Pt I
Pt I
Ni I
HD 122563
HD 115444
HD 126238

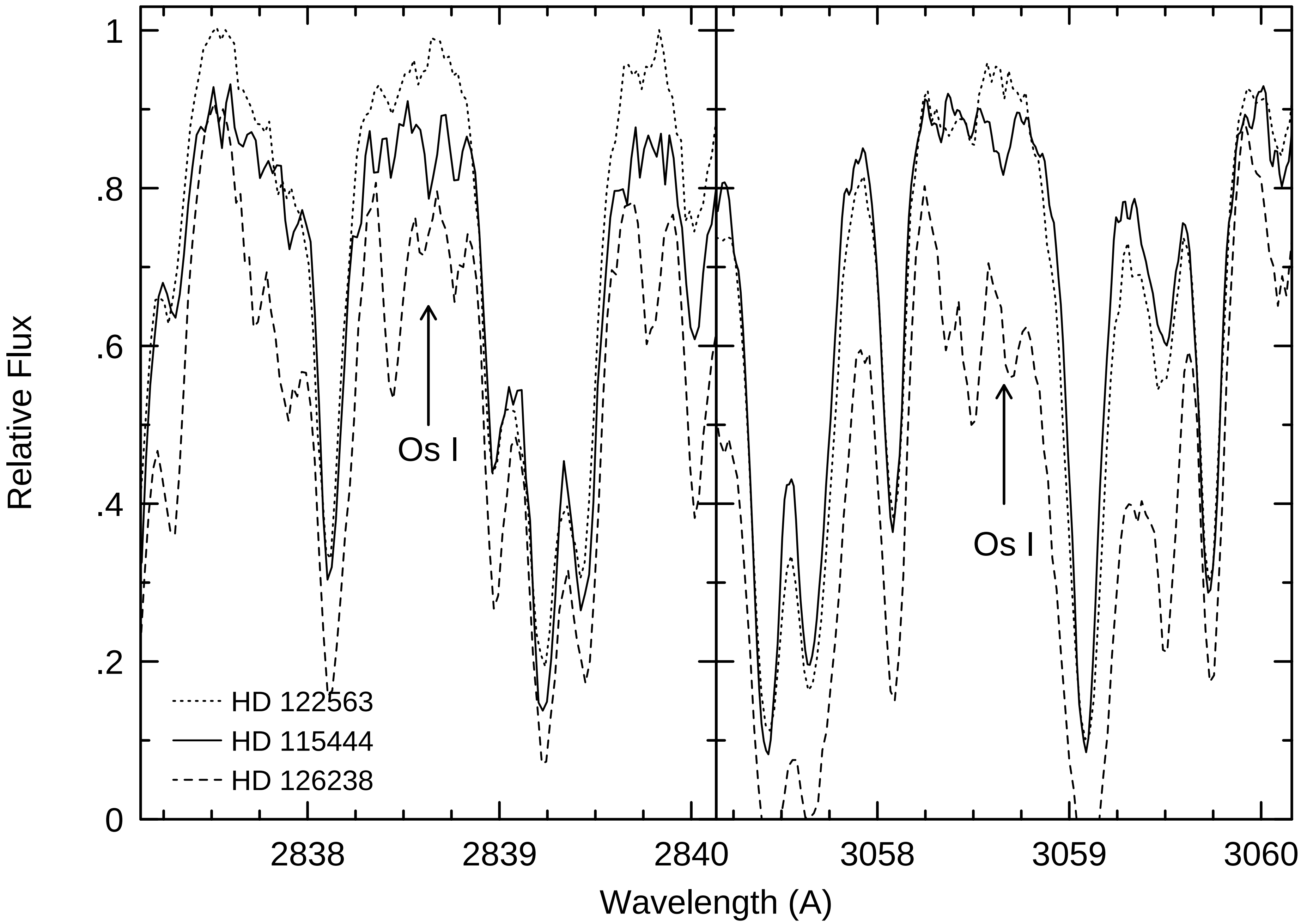

Relative Flux
1
.8
.6
.4
.2
0
2838
2839
2840
3058
3059
3060
Wavelength (A)
Os I
Os I
HD 122563
HD 115444
HD 126238

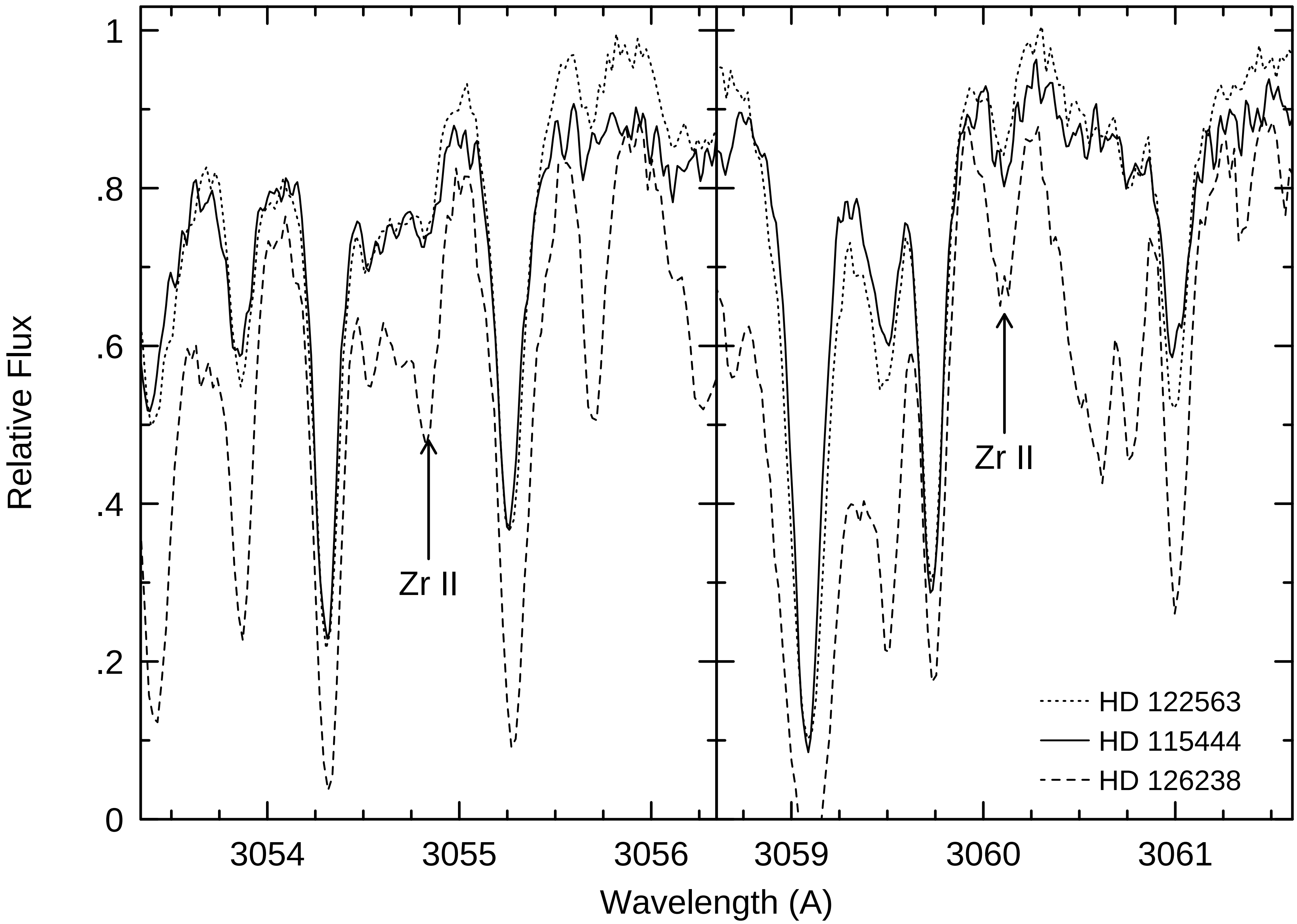

Relative Flux
1
.8
.6
.4
.2
0
3054
3055
3056
3059
3060
3061
Wavelength (A)
Zr II
Zr II
HD 122563
HD 115444
HD 126238

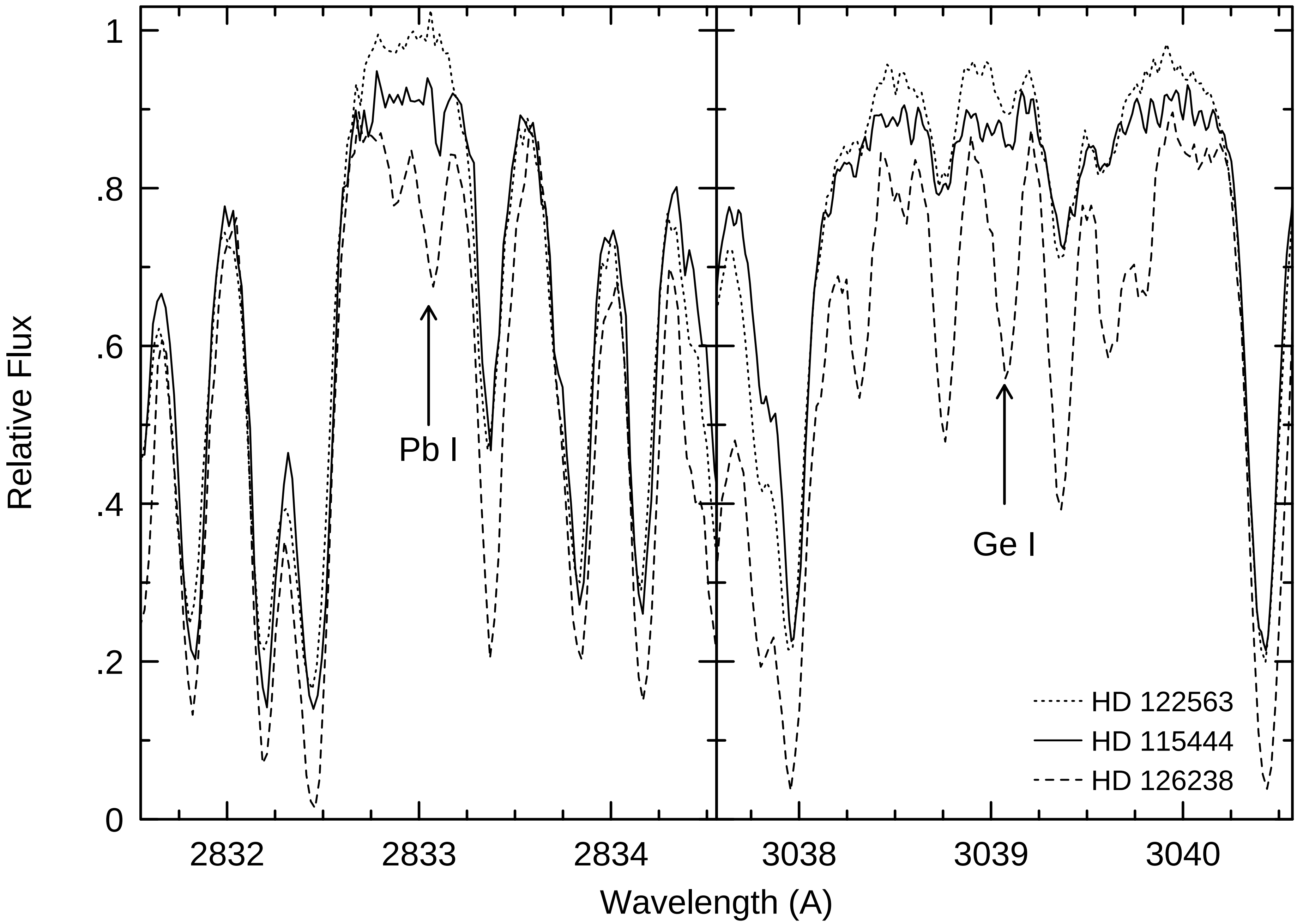

Relative Flux
0
.2
.4
.6
.8
1
2832
2833
2834
3038
3039
3040
Wavelength (A)
Pb I
Ge I
HD 122563
HD 115444
HD 126238

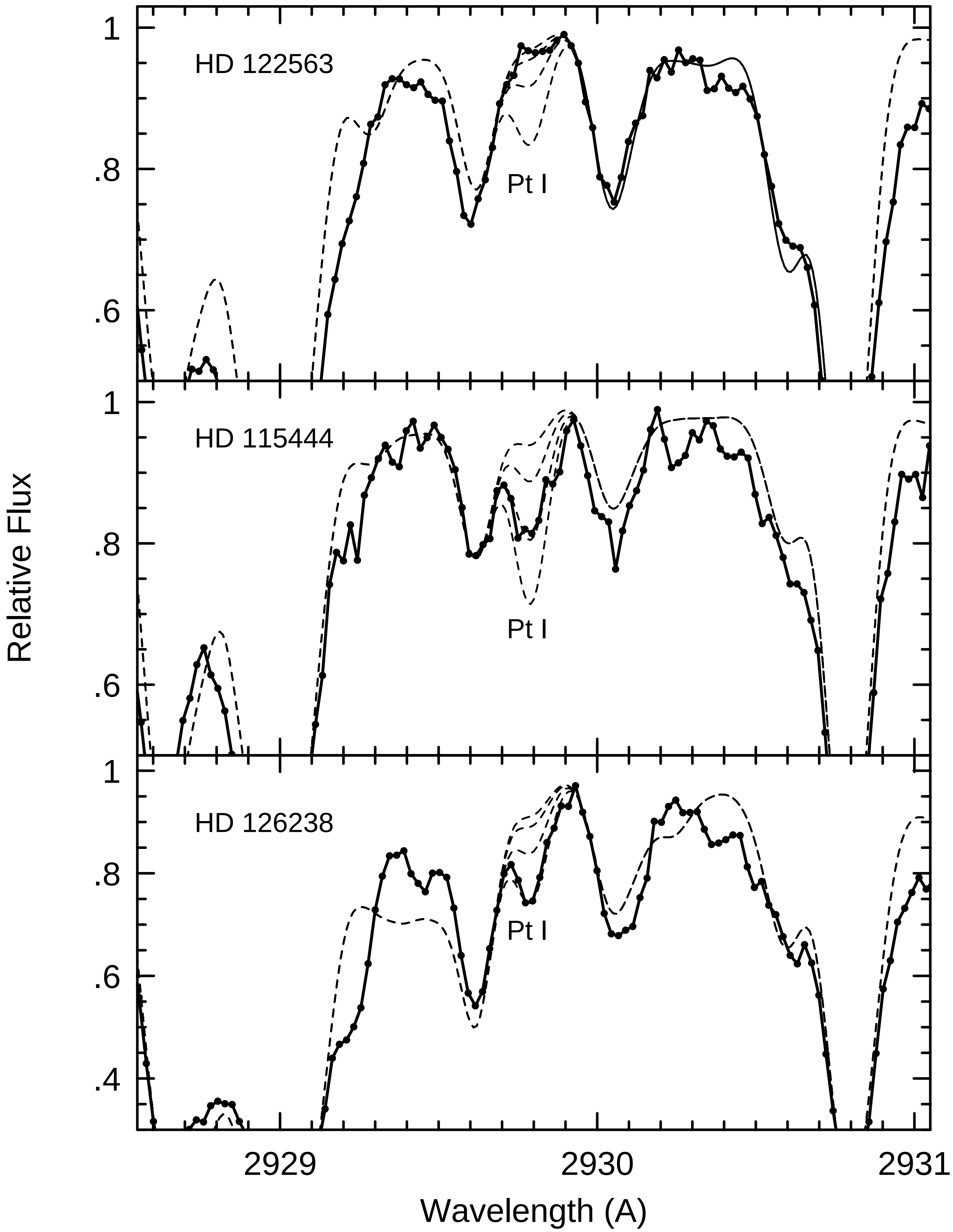

HD 122563
HD 115444
HD 126238
Pt I
Pt I
Pt I
1
.8
.6
.4
2929
2930
2931
Relative Flux
Wavelength (A)

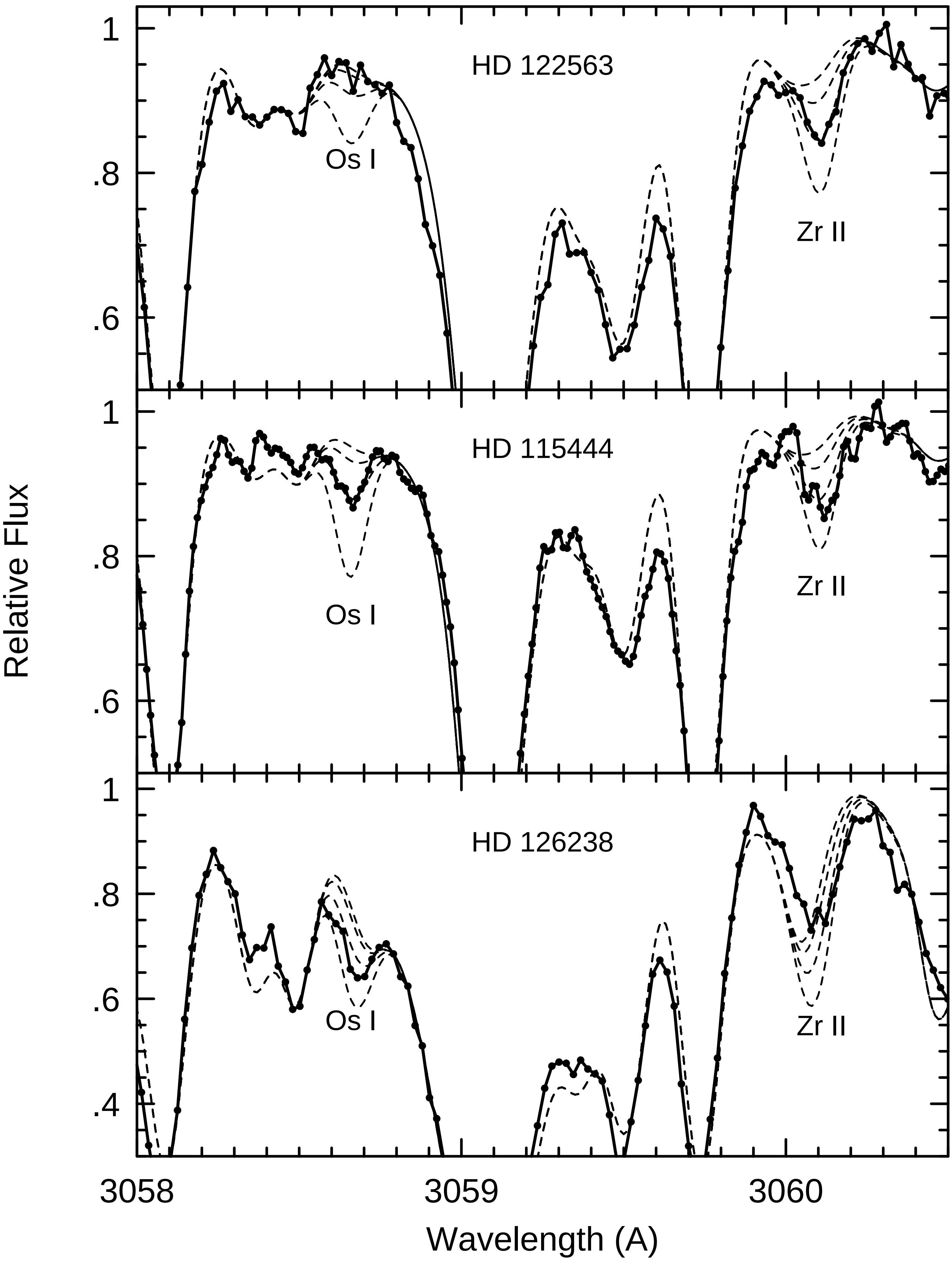

HD 122563
Os I
Zr II
HD 115444
Os I
Zr II
HD 126238
Os I
Zr II
Relative Flux
Wavelength (A)
1
.8
.6
.4
3058
3059
3060

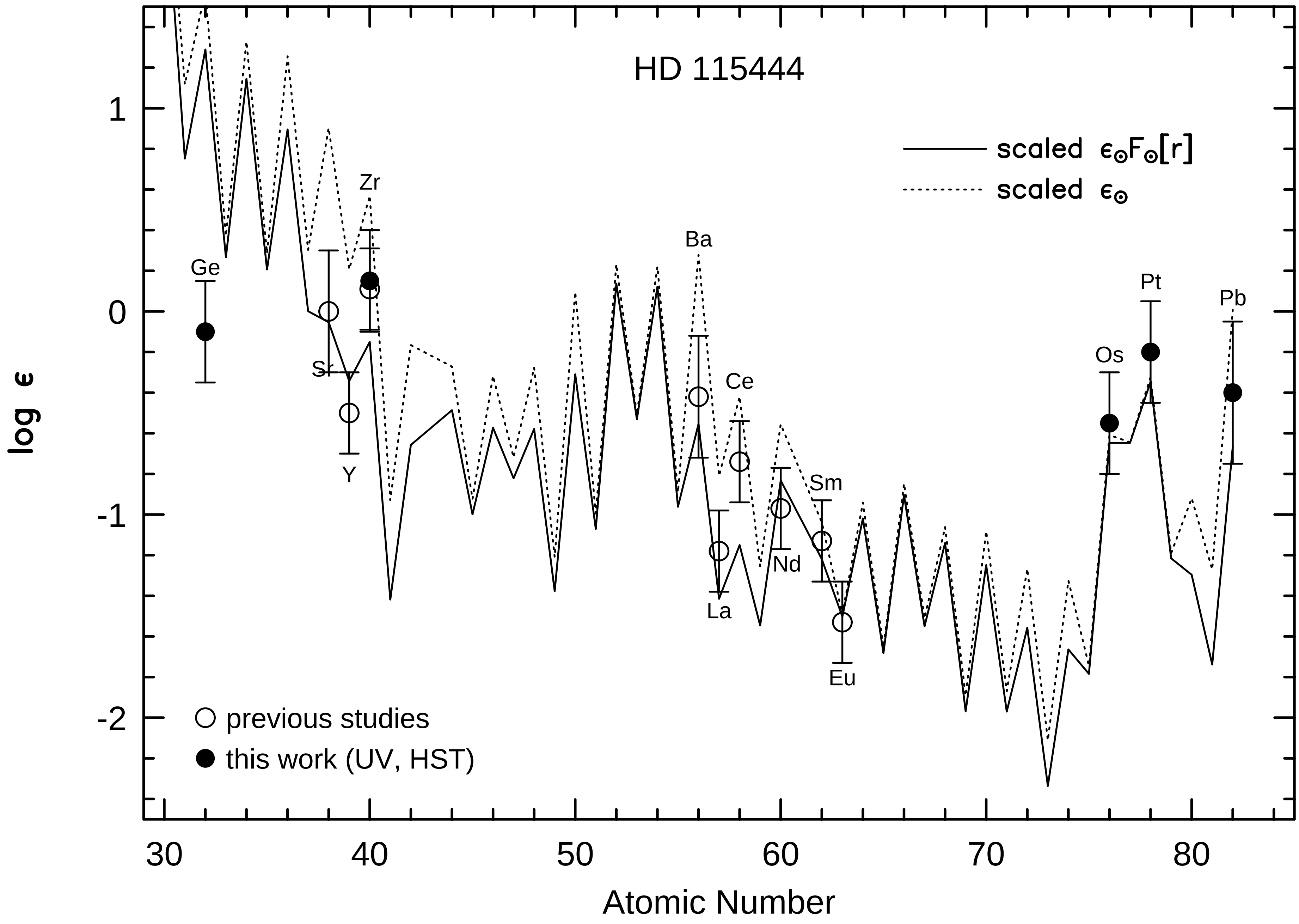

HD 115444
scaled $\epsilon_\odot F_\odot[r]$
scaled $\epsilon_\odot$
previous studies
this work (UV, HST)
log ε
Atomic Number
Ge
Sr
Y
Zr
Ba
La
Ce
Nd
Sm
Eu
Os
Pt
Pb
1
0
-1
-2
30
40
50
60
70
80

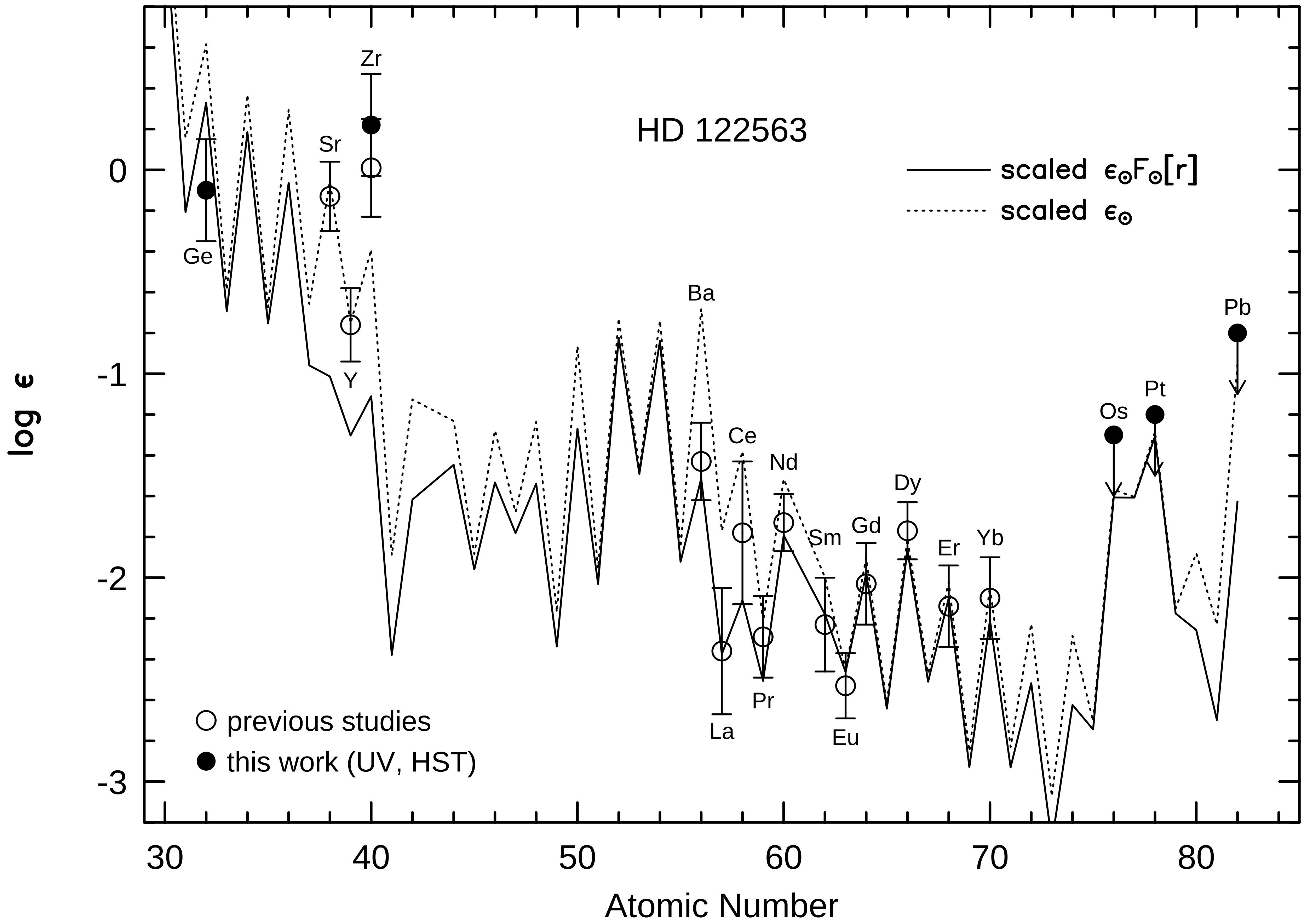
HD 122563
scaled ε⊙F⊙[r]
scaled ε⊙
previous studies
this work (UV, HST)
log ε
Atomic Number
0
-1
-2
-3
30
40
50
60
70
80
Ge
Sr
Zr
Y
Ba
Ce
Nd
La
Pr
Sm
Eu
Gd
Dy
Er
Yb
Os
Pt
Pb

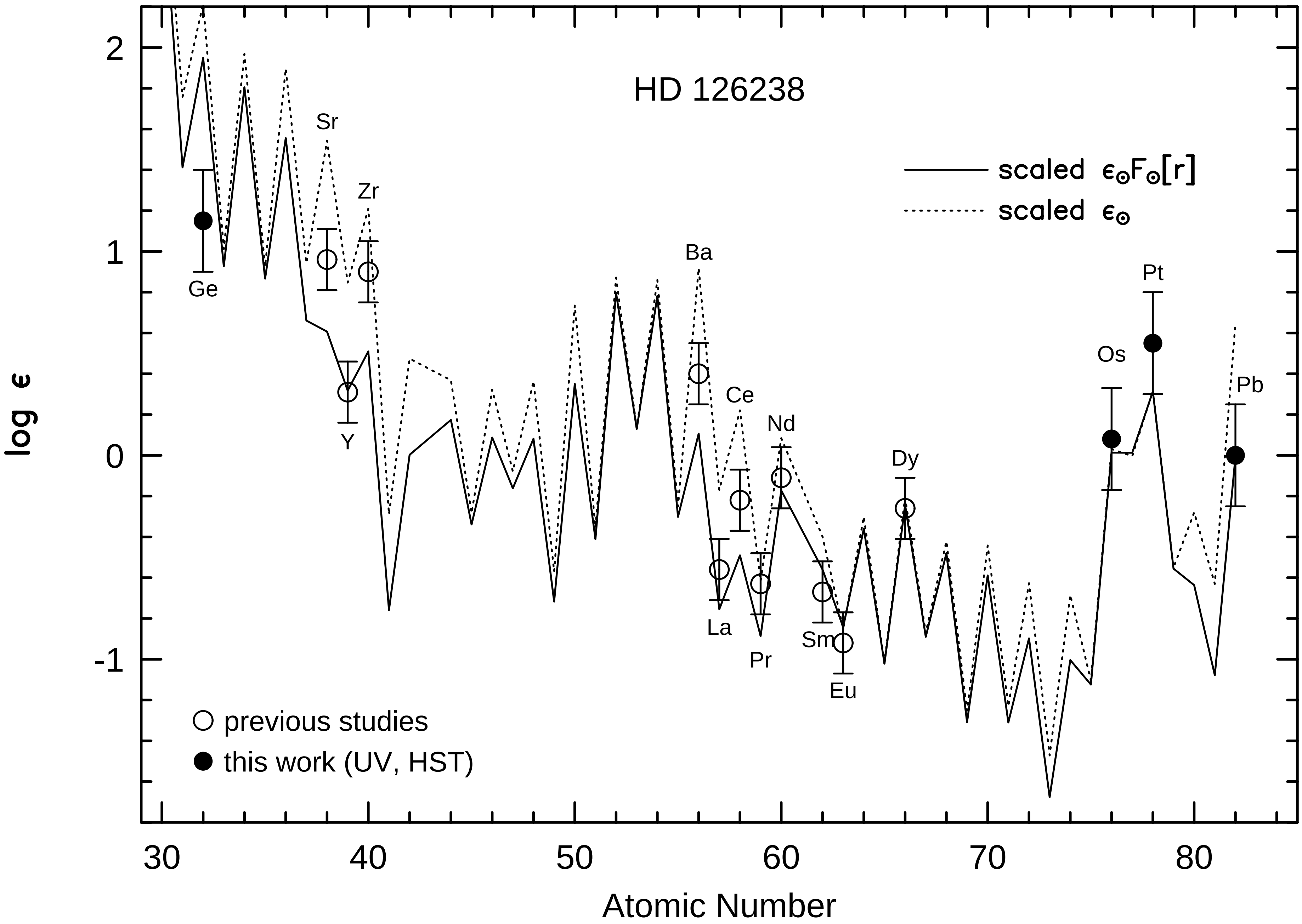

HD 126238
scaled ε⊙F⊙[r]
scaled ε⊙
previous studies
this work (UV, HST)
log ε
Atomic Number
Ge
Sr
Zr
Y
Ba
Ce
La
Pr
Nd
Sm
Eu
Dy
Os
Pt
Pb
2
1
0
-1
30
40
50
60
70
80